Supporting Information

Plasmonic Heating Induced by Au Nanoparticles for Quasi-ballistic Thermal Transport in Multi-walled Carbon Nanotubes

Yanru Xu[1a], Xiaoguang Zhao[2a], Aobo Li[2], Yanan Yue[1,2], Jin Jiang[1], Xin Zhang[2,*]*

[1]Key Laboratory of Hydraulic Machinery Transients (MOE), School of Power and Mechanical Engineering, Wuhan University, Wuhan, Hubei 430072, China
[2]Department of Mechanical Engineering, Boston University, Boston, Massachusetts 02215, USA
[a] These authors contribute equally.

To whom the correspondence should be addressed: Y.Y.: yyue@whu.edu.cn; X. Z.: xinz@bu.edu

1. Simulation details

As shown in Fig. S1a, in the simulation model, a hexagonal array of Au cylinders is used for representing the array of Au nanoparticles (AuNPs) on silicon. According to SEM image (see Fig. S1b), the cylinders' diameter is 30 nm and their height is 20 nm corresponding to the real samples. The array periodicity is 65 nm. Simulation region is 730 × 782 × 1500 nm^3 ($x \times y \times z$). Periodic boundary conditions are used in the x-y plane and perfectly matched layer boundary conditions on z direction. The distance from the AuNPs to the absorbing boundary is set to be larger than one half of the incident wavelength. The entire domain is adaptively divided into cuboid elements with their length of side less than 1/26 of the incident wavelength. A set of plane waves (400 nm to 800 nm) is incident along the negative direction of z axis polarized along the x axis. The amplitude of the incident electric field (E_0) is set to be 1 V m^{-1}. In the calculation of power absorption, the incident amplitude of 1.08×10^5 V m^{-1} (corresponding to the intensity of 0.015 mW μm^{-2}

used in the experiment) is used. The permittivity of gold is from data reported by Johnson and Christy.[1] The dielectric constant of silicon is taken from the literature.[2] The calculated Raman enhancement factor is estimated as the second power of electric intensity enhancement factor based on the electromagnetic enhancement mechanism.[3, 4] The power absorption per volume ($\dot{q}_{\mathrm{Au}}$) is calculated using the expression of $\dot{q}_{\mathrm{Au}} = 0.5\varepsilon_0\omega\mathrm{Im}[(\varepsilon(\omega)]E_{\mathrm{loc}}^{\ 2}$, where ε_0 is the vacuum permittivity, ω is the angular frequency of the incident wave, Im[$\varepsilon(\omega)$] is the imaginary part of the permittivity of Au at the incident frequency of ω and E_{loc} is the amplitude of the local electric field derived from electromagnetic simulations.[5] Absorbed power in a single AuNP (q_{Au}) is obtained by integration of power absorption per unit volume ($\dot{q}_{\mathrm{Au}}$) throughout single AuNP and averaging within the simulated array of AuNPs.

2. Validation of surface plasmon property of AuNPs

In this work, we choose Raman-active silicon wafer as the substrate because it can be used directly to validate the Raman enhancement effect of AuNPs, also it can act as an excellent heat sink for thermal transport. However, bulk silicon is not transparent over the visible range like glass, quartz or sapphire substrate, which makes the UV-vis absorption spectroscopy measurement difficult. Therefore, we calculate the extinction curve of AuNPs with finite-difference time-domain (FDTD) simulations. To obtain the extinction (absorption, A), we simulate the reflection (R) and transmission (T), and calculate the extinction by A=1 – R – T. The calculated results of our sample are shown as below (Fig. S2).

Fig. S2 shows that AuNPs exhibit an extinction band in the range of 400 nm to 800 nm with a peak wavelength at 561 nm. In Huang et al' work[3], they used anodic aluminum oxide (AAO) template to prepare Au nanorod arrays with diameter of 30 nm and gap of 30 nm. The measured UV-vis spectrum of the Au nanorod arrays showed plasmon resonance peak at 513 nm. In comparison, our calculated extinction spectrum of AuNPs agrees well with their measured results. By comparing our calculated extinction spectrum with the reported results, the plasmon property of our AuNPs could be validated in combination with Raman enhancement measurement.

3. Evaluation of size deviation effects on calculated electric intensity enhancement

The diameter and the periodicity of AuNPs are important parameters in this work. Based on the SEM image of AuNPs as shown below (Fig. S1b), we statistically studied the distribution of particle size and periodicity. The average diameter and periodicity of AuNPs with standard deviations are 30.2 ± 4.1 nm and 64.6 ± 2.4 nm, respectively. To evaluate the effects of their deviations on the electric field intensity enhancement, numerical simulations on the electric field around AuNPs considering the standard deviations are performed. The periodicity of AuNPs is first fixed at 65 nm. The electric field around AuNPs with diameter of 26 nm, 30 nm and 34 nm are simulated, respectively. The electric intensity enhancement factors in the range of 400 nm to 800 nm are shown in Fig. S3a. In comparison, the enhancement factors of these diameters exhibit similar bands. As the diameter increases, the peak wavelength redshifts slightly, in agreement with a previous report on plasmonic band of gold nanodisk[6]. The shift of peak value is lower than 6% as diameter increases

from 26 nm to 30 nm or from 30 nm to 34 nm. At 532 nm, the corresponding enhancement factor shows a negligible reduction as diameter varies.

Then, the diameter of AuNPs is fixed at 30 nm in the models. The electric field around AuNPs for periodicity of 63 nm, 65 nm and 67 nm are simulated, respectively. Electric intensity enhancement factors over the range of 400 nm to 800 nm are shown in Fig. S3b. The difference in the frequency responses for different periodicities of the AuNPs is negligible. At 532 nm, the corresponding enhancement factors are almost the same for AuNPs with periodicities of 63 nm, 65 nm and 67 nm. These simulation results show that the little variations of diameter and periodicity in our work will not impact the calculated electrical intensity enhancement for the designated structure.

In order to evaluate the defect effects on the calculated electric intensity enhancement, we perform electromagnetic simulations on AuNPs considering defect ratio from 10% to 50% using FDTD simulation models similar as described in Section 1. A top view of the model is shown in the right inset of Fig. S4a, in which the gray circles represent where AuNPs is absent, the orange circles represent the undamaged AuNPs and the yellow rectangle represents the simulation region. Fig. S4a shows that Raman enhancement of AuNPs decreases with the defects of Au NPs increase. The peak wavelength change is negligible as the defect ratio increases. Compared with the perfect AuNP array, Raman enhancement factor decreases by 8% if 10% defect exists at excitation of 532 nm laser, as shown in Fig. S4b. When the defect ratio is 50%, Raman enhancement decreases by 44%. It could be concluded that our experimental Raman enhancement factor that is much lower than the calculated one is ascribed to the defect of AuNPs.

4. Laser heating experiment details

MWCNTs are distributed randomly on the AuNPs/Si and bare silicon substrates, respectively. They agglomerate due to the van der Waals forces. The agglomeration results in a non-uniform thickness in the MWCNTs layer and may have caused experimental uncertainties which need to be carefully addressed. The locations with similar thickness of MWCNTs are determined at first. Since it is difficult to measure the MWCNTs thickness directly, we use peak intensity of D-band and Si-band to monitor the MWCNTs thickness variation.[7] Multiple scannings indicate that the distribution of MWCNTs is full of ups and downs revealed by the observation that the peak intensity of Si-band falls (or rises) and that of D-band rises (or falls) for continuous scanning on MWCNTs/AuNPs/Si sample and the control group under the same focal levels. We take two sets of scanning on the samples for example. As shown in Fig. S5, we scan the control group for two times, denoted as P1 and P2. P3 and P4 represent the two sets of scanning on the sample. Peak intensity of Si-band vs. that of D-band indicates that there are regions on two samples with overlapped signals in which peak intensity of D-band ranges from 2900 to 5600 and peak intensity of Si-bandd from 42400 to 29700. Therefore, we select the points on P1 and P3 with similar D-band peak intensity as the sites which are fixed to be monitored in the heating experiment. Raman spectra of fixed locations on the sample and the control group are shown in Fig. S6. The lower inset of Fig. S6 shows that, between the MWCNTs/AuNPs/Si sample and the control group, peak intensity of D-band intensity differs by 5%. Considering the optical enhancement of AuNPs, Raman signals of the two fixed locations are considered reasonable and comparable.

In order to evaluate temperature rise of silicon, Raman calibration of temperature coefficient is performed over a temperature range from 294 K to 364 K as shown in the inset of Fig. S7. As temperature increases, peak frequency of Si-band shifts to lower wavenumber. The fitted slope for the peak position of Si-band versus temperature is –0.023 cm^{-1} K^{-1}, as shown in Fig. S7, agreeing well with the reported values (–0.0201~–0.0247 cm^{-1} K^{-1}).[8-10]

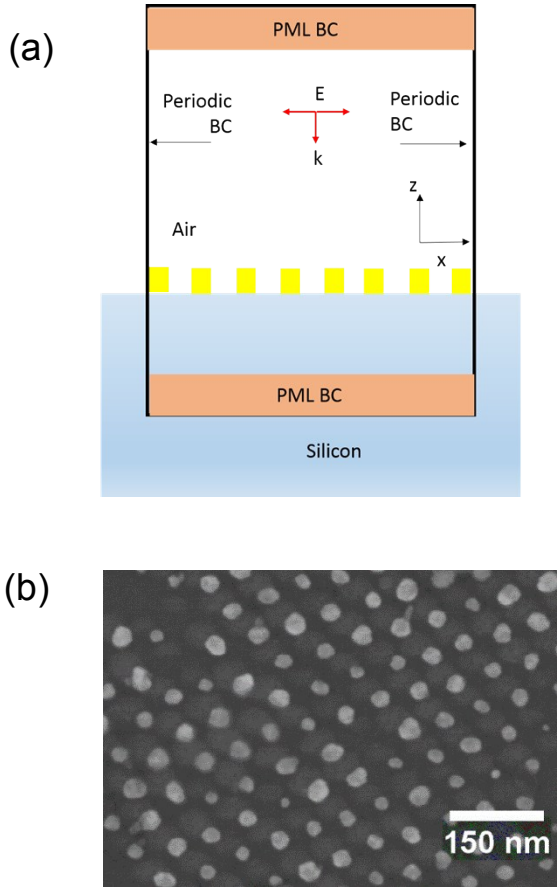

Fig. S1. (a) Schematic of the simulation model. (b) An SEM image of AuNPs array on silicon.

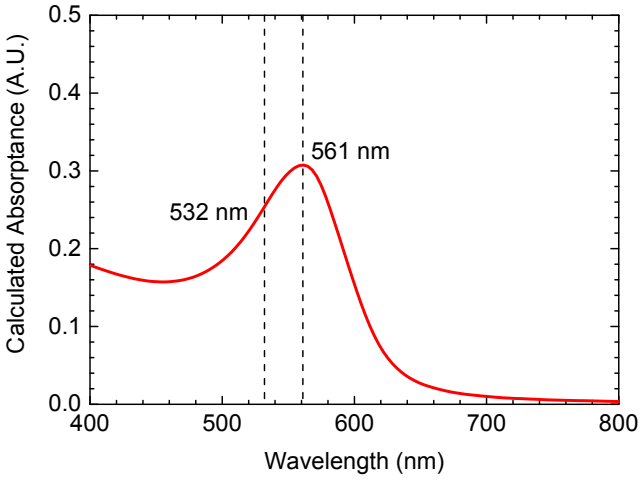

Fig. S2. The simulated extinction curve of AuNPs.

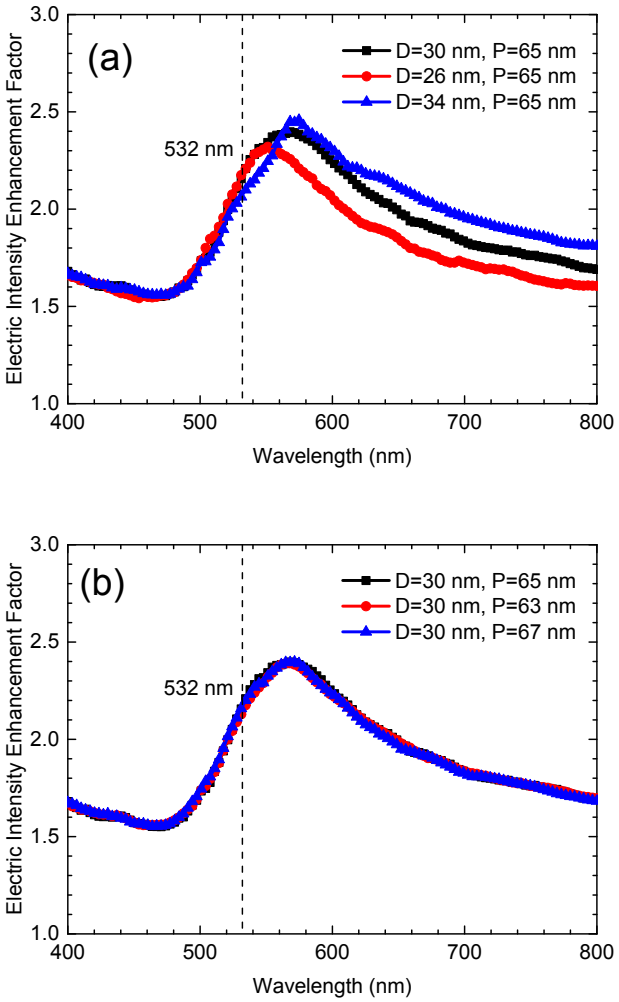

Fig. S3. (a) The calculated electric intensity enhancement factor as a function of wavelength for AuNPs with various diameters considering the standard deviation. The periodicity of particles is fixed at 65 nm. (b) The calculated electric intensity enhancement factor as a function of wavelength for AuNPs with various periodicities considering the standard deviation. The diameter of particles is fixed at 30 nm.

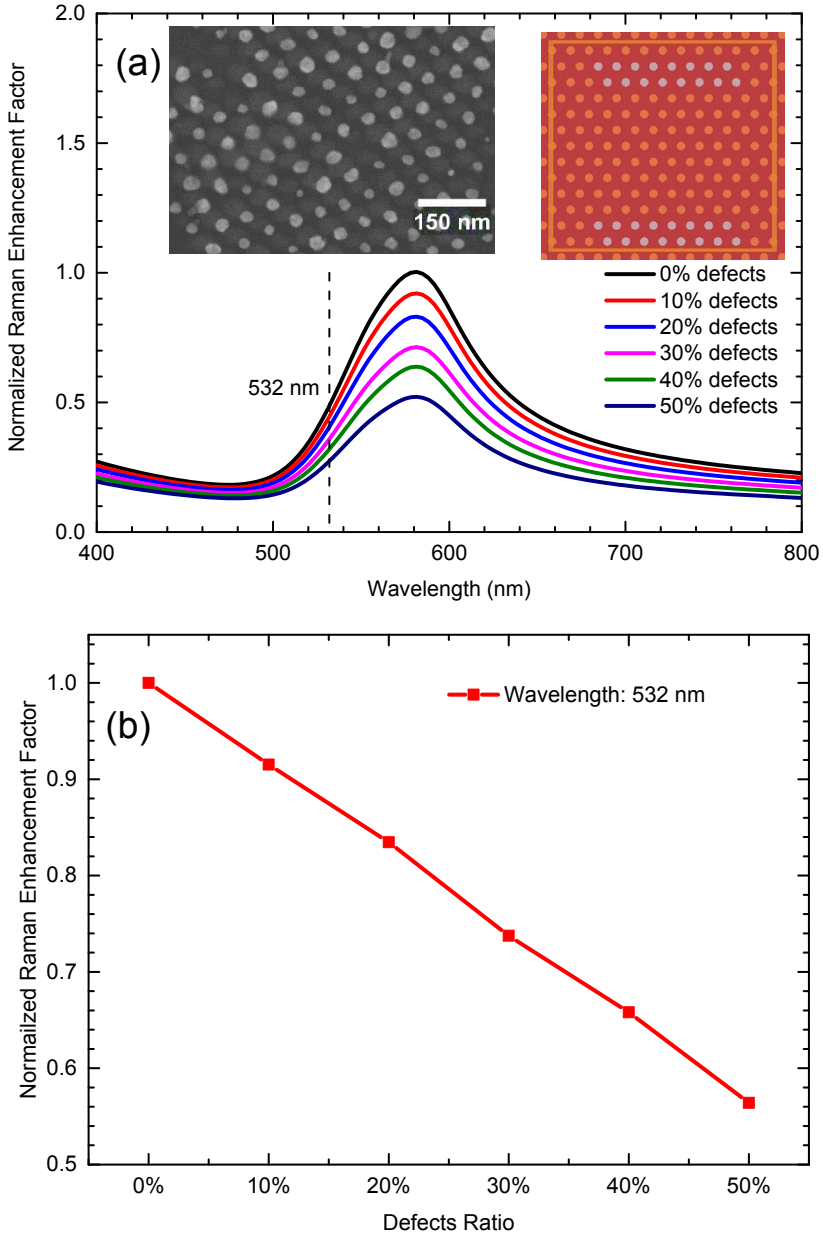

Fig. S4. (a) Raman enhancement factor as a function of wavelength for AuNPs with (10-50%) and without defects. All results are normalized to the peak value of spectrum for 0% defects. The left inset is a SEM image of AuNPs. The right inset is a top view of simulation model with defects, in which the gray dots represent the missing particles. (b) Raman enhancement factor of AuNPs with (10-50%) and without defects at excitation of 532 nm laser. All results are normalized to the one for 0% defects.

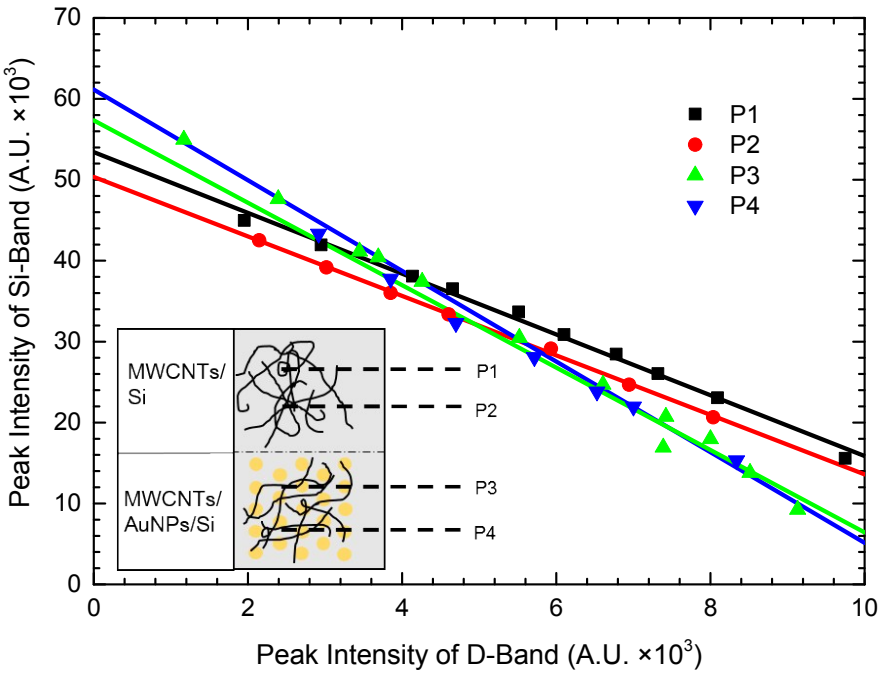

Fig. S5. Peak intensity relationship between Si-band and D-band. The integration time is set to be 1 minute.

The inset depicts the scanning sets of P1 to P4 on the MWCNTs/AuNPs/Si sample and the control group.

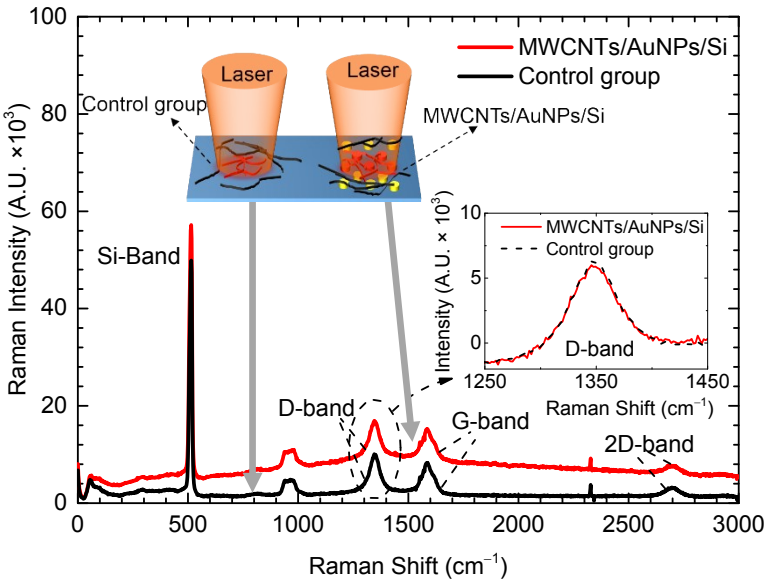

Fig. S6. Raman spectra of MWCNTs/AuNPs/Si and the control group for targeting measurement locations. The lower inset depicts that peak intensity of D-band for the sample is similar as that of the control group. The upper inset illustrates a schematic of laser heating on the sample and the control group.

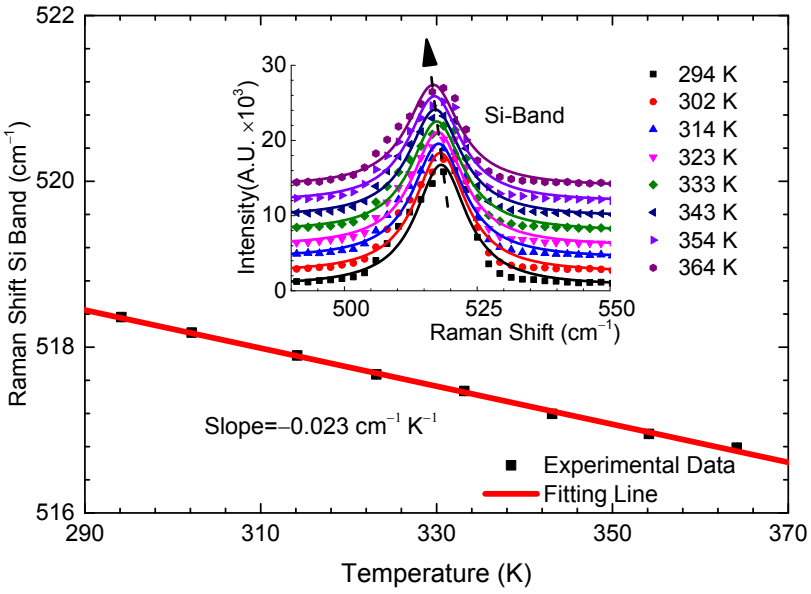

Fig. S7. Calibration result for peak position of Si band vs temperature.

Notes and references

1 P. B. Johnson and R. W. Christy, *Phys. Rev. B*, 1972, **6**, 4370-4379.

2 D. F. Edwards, in *Handbook of Optical Constants of Solids*, Academic Press, Burlington, 1997, 547.

3 Z. Huang, G. Meng, B. Chen, C. Zhu, F. Han, X. Hu and X. Wang, *J. Nanosci. Nanotechnol.*, 2016, **16**, 934-938.

4 M. Moskovits, *J. Raman Spectrosc.*, 2005, **36**, 485-496.

5 G. Baffou, R. Quidant and C. Girard, *Appl. Phys. Lett.*, 2009, **94**, 153109.

6 A. E. Schlather, N. Large, A. S. Urban, P. Nordlander and N. J. Halas, *Nano Lett.*, 2013, **13**, 3281-3286.

7 A. Duzynska, M. Swiniarski, A. Wroblewska, A. Lapinska, K. Zeranska, J. Judek and M. Zdrojek, *Carbon*, 2016, **105**, 377-386.

8 J. Menéndez and M. Cardona, *Phys. Rev. B*, 1984, **29**, 2051-2059.

9 H. H. Burke and I. P. Herman, *Phys. Rev. B*, 1993, **48**, 15016-15024.

10 X. Tang, S. Xu, J. Zhang and X. Wang, *ACS Appl. Mater. Interfaces*, 2014, **6**, 2809.